A 1.25-Gb/s Indoor Cellular Optical Wireless Communications Demonstrator

Hoa Le Minh, Dominic O'Brien, Grahame Faulkner, Olivier Bouchet, Mike Wolf, Liane Grobe, and Jianhui Li

***Abstract*—This letter reports an experimental demonstration of an indoor angle-diversity optical wireless communications system. This operates at 1.25 Gb/s and provides bidirectional communications between two terminals. Each terminal uses three transmitting "cells" giving a field of view of approximately $25^\circ \times 8^\circ$ over a range of approximately 3 m. Data is transmitted to a terminal that uses three receivers to obtain a similar reception field of view. Link operation at a bit-error rate $< 10e$-9 is reported, together with an overview of the system configuration.**

***Index Terms*—Infrared (IR), optical wireless, wireless communications.**

I. Introduction

THE deployment of fiber to the home and ultrafast broadband will bring data rates of 100s of megabits per second to the home, and to fully utilize these home access networks (HANs) that provide gigabits per second, class connectivity will be required. A European Community project "Home Gigabit Access Network" (OMEGA) aims to achieve this, using a variety of wireless and wired techniques [1]. This heterogeneous approach is likely to be increasingly important as the number and variety of different wireless devices increases.

Part of this project is to investigate optical wireless communications, using visible light communications (VLC) to broadcast information [2], and infrared (IR) optical wireless communications to provide high-speed line-of-sight connections to the home area network. This letter focuses on the IR line-of-sight system. Line-of-sight architectures are often used for very high-speed systems, and narrow field of view free space optical (FSO) links operating over several kilometers at gigabit rates have been demonstrated [3]. Indoor optical wireless requires high data rates and wide field of view (FOV) to achieve coverage, while maintaining eye safety. This requires the use of multiple transmitters and multiple receivers, and these are usually arranged using imaging [4] or angle diversity [5] configurations. In this case, an angular diversity configuration was preferred, as it allows the use of commercially available components, rather than custom arrays of devices, as used, for example, in [6].

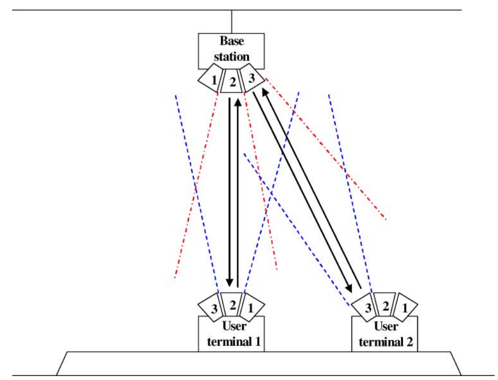

Fig. 1. One-dimensional optical wireless cellular system.

Fig. 1 shows a schematic of the system which contains a base station (BS) and a number of user terminals (UTs) which have identical physical layer components. The BS transmitter consists of three separate channels arranged to give continuous angular coverage of a field approximately $25^\circ \times 8^\circ$ in extent. Each UT has three receiver channels, each of which has a field of view matched to a transmitter channel. Together these create an overall reception field of view matching that of the BS transmitter. This system of three transmitter and receiver channels forms a "downlink" from the BS to UT. As the UTs move within the coverage area, they fall within the coverage of different transmitter channels, so some control mechanism is required to ensure the correct receiver and transmitter channels are active. For this demonstration, all BS transmitter channels send the same data and are always on, and a thresholding mechanism is used at the UT to select the individual receiver channel that is detecting the transmitted data. This is the simplest scheme that allows system operation with one BS and UT, and work by other partners in the OMEGA project is concerned with implementing a full optical wireless medium access control (MAC) layer [7] that would allow multiple terminals to operate. The "uplink" from UT to BS operates independently of the "downlink" and uses an identical set of components and control mechanisms.

In Sections II–IV the system components, operation and results are described.

Manuscript received April 01, 2010; revised August 24, 2010; accepted August 27, 2010. Date of publication September 07, 2010; date of current version October 13, 2010. This work was supported by the European Community's Seventh Framework Programme FP7/2007-2013 under grant agreement n ° 213311, also referred to as OMEGA. This information reflects the consortium's view, and the Community is not liable for any use that may be made of any of the information contained therein.

H. Le Minh, D. O'Brien, and G. Faulkner are with the Department of Engineering Science, University of Oxford, Oxford OX1 3PJ, U.K. (e-mail: dominic.obrien@eng.ox.ac.uk).

O. Bouchet is with France Telecom, Cesson-Sévigné, Rennes, Paris 75015, France.

M. Wolf, L. Grobe, and J. Li are with the Communications Research Laboratory, University of Ilmenau, llmenau 98693, Germany.

Color versions of one or more of the figures in this letter are available online at http://ieeexplore.ieee.org.

Digital Object Identifier 10.1109/LPT.2010.2073696

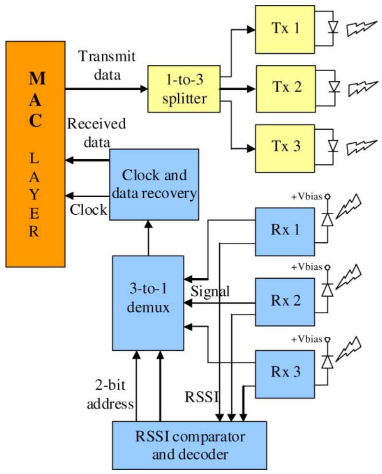

Fig. 2. Functional block diagram of a base-station/user-terminal unit.

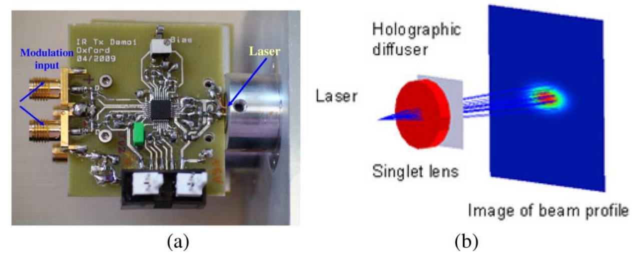

Fig. 3. (a) Transmitter laser driver and (b) optics subsystem.

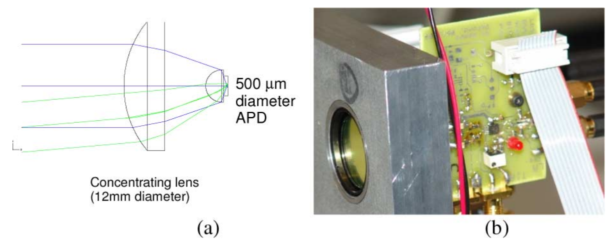

Fig. 4. (a) Receiver optics ray-tracing design and (b) receiver prototype.

II. System Description

A. System Description

Fig. 2 shows the functional block diagram of the physical layer (PHY) of the proposed BS (or UT as they are identical).

Transmit data from the MAC is split and used to modulate the IR beams emitted from the transmitter lasers (shown as Tx1,2,3 on the diagram). All transmitters transmit the same data and are always active. This light propagates to the receiving terminal.

The receiver subsystem (Rx1,2,3) is also shown on the diagram and consists of three receivers which collect the received optical power, and recover a binary electrical signal from it. Each receiver provides a "received signal strength indicator" (RSSI) signal to allow the "active" receiver to be determined. This is set to "high" when the received signal has its power level greater than a predefined threshold (at which the signal bit-error rate (BER) is $\leq 10^{-9}$). Decision circuitry controls a demultiplexer which will route that received signal to a clock and data recovery (CDR) module which forwards the recovered data to the MAC. In the case where two receivers have their RSSI values greater than the threshold (which might happen at the overlapped region of two cells), the one with the lower given index number (e.g., Rx1 has a lower given index number than Rx2) will be selected. This might be called "Select Good Enough" and is inferior compared with Maximal Ratio Combining or Select Best, but a simple priority encoder integrated circuit can be used to implement this strategy, so it was sufficient for this initial demonstration.

In Sections 2-B and 2-C, the transmitter and receiver components are described.

B. Transmitter Design

Fig. 3(a) shows a single transmitter channel and Fig. 3(b) shows a modeling of the optical system. The transmitter consists of a driver, laser, and optics system. A commercial (MAX3869) laser driver is used to modulate a single-mode 820-nm laser (AXCEL PHOTONICS), which emits an average communications optical power of 25 mW. The optical system is used to collimate the laser and illuminate a commercial holographic diffuser (LUMINIT 10° LSD). The diffuser renders the source class 1 eye-safe and spreads the illumination within the desired 10° transmitter field of view.

C. Receiver Design

The receiver consists of an optical filter, collection optical system, avalanche photodetector (APD), and transimpedance amplifier followed by a limiting amplifier. Fig. 4(a) and (b) shows the receiver optical system and a prototype receiver, respectively. An interference filter with an optical bandwidth of 10 nm is used to reject ambient light before entering the optical system, which consists of two plano-convex lenses. These collect light and focus it onto the receiver APD. The maximum optical "gain" (defined as the ratio of the collection area to the detection area) is set by the desired FOV ($\sim 8° - 10°$ full angle) and limited by constant radiance considerations. In this case, only commercial lenses were available, and an estimated on-axis optical gain of 300, about 65% of theoretical maximum (assuming a glass refractive index of 1.5) was achieved. A commercial APD and transimpedance amplifier in receiver-optical subassembly (ROSA) form (AD500-1.3G-TO5) was used, with a 0.5-mm diameter APD. The overall optoelectronic bandwidth is approximately 850 MHz, with a measured sensitivity of -35 dBm for nonreturn-to-zero (NRZ) data transmission at 1.25 Gb/s for a BER below 10^{-9}.

D. Decision Circuitry

As mentioned in the system description, a "Select Good Enough" approach is used at the receiving terminal. The signal from each ROSA is fed into a limiting amplifier to obtain logic level outputs. In addition, a threshold detection output is available, and this is used to indicate received signals high enough to recover good data. These signals are used as inputs to a priority encoder (74LS148) that selects the appropriate output of a multiplexer (MAX9386).

III. Experimental Results

A system consisting of one BS and one UT was fabricated. A pseudorandom bit-stream (PRBS) $2^{15}-1$ data source was used

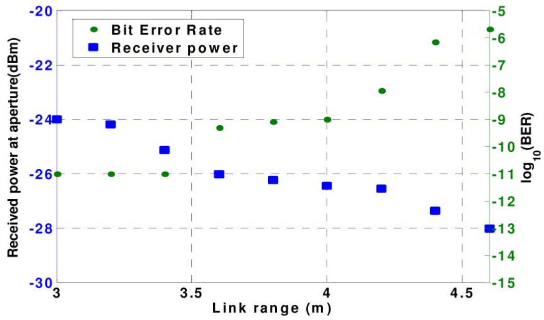

Fig. 5. (Left) Received optical power and (right) BER against link range.

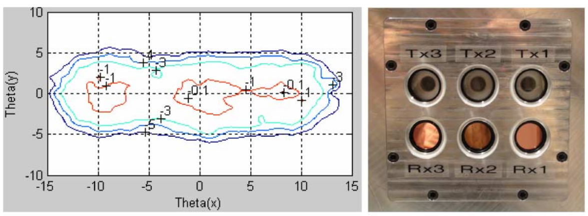

(a) (b)

Fig. 6. (a) Measured received power distribution versus angle. (b) Front face of user terminal.

TABLE I
LINK BUDGET AT CELL CENTER

Transmitted average communications power	+14dBm
Received intensity at 3m	-23dBm/cm^2
Estimated collection area (on-axis)	0.63 cm^2
Available power	~-25dBm
Inferred additional receiver loss (Simulated additional loss ~3.3dB)	~7dB
Available APD received sensitivity	~35dBm
Measured system margin	~3dB

to test the system. Fig. 5 shows the BER performance against the on-axis link range, showing error-free operation $(\mathrm{BER} < 10^{-9})$ up to 4 m, together with the power collected at the receiver entrance aperture. The reduction in received power density is approximately -2.7 dB when the range is increased from 3 to 4 m, indicating the system has an operating margin of approximately 3 dB at the desired 3-m range. A plot of the relative received power with angle for the system is shown in Fig. 6(a). This is derived from the measured transmitter emission patterns and the measured receiver collection characteristics, and shows an FOV of approximately $25^\circ \times 8^\circ$ using the -3-dB contour (corresponding to the system margin) as the edge of the coverage area. At the desired operating range of 3 m, this corresponds to an area of 1.3 m $\times$ 0.45 m. Measurements of the BER within the coverage area were made, by translating the UT relative to the BS, and these remained below 10^{-11}. Fig. 6(b) shows the front face of a terminal, with transmitters and receivers visible.

Table I shows the link budget for the system. The measured overall margin is 3 dB, as mentioned earlier, but there are unaccounted losses of approximately 4 dB compared with simulation. These are likely to be due to misalignment in the receiver optical system and additional noise in the thresholding and decision circuitry (which is not taken into account in the receiver sensitivity measurement). Work to reduce these is ongoing.

A 3.4-m link was established and the UT was directed to an open window on a bright sunny day (without direct sunlight) and an on-axis incandescent lamp. The total luminous intensity measured at the UT is 1200 lux (a typical minimum level for a well-lit office is approximately 400 lux). The measured BER increased from a level below 10^{-11} (without incandescent lighting) to 10^{-9} showing that the system is robust. The BER increase corresponds to an additional noise current of $\sim$14 nA, which is due to the additional shot-noise caused by the direct current (dc) photocurrent from the ambient illumination. This value is in good agreement with that expected from estimations using the measured spectra of these ambient sources. Bidirectional data transmission was also implemented between BS and UT. These were both connected to personal computers (PCs) via field programmable gate array (FPGA) boards acting as the media converters. Video streaming over these links in both directions was reliably demonstrated.

IV. DISCUSSION AND CONCLUSION

This letter reports the operation of a 1-D angle diversity optical wireless system at 1.25 Gb/s, the fastest demonstration of its type to the best of our knowledge. Spectrum scarcity means that RF wireless systems are moving to higher carrier frequencies, where propagation is close to, or line of sight. In such circumstances optical wireless may offer a low latency, energy efficient alternative using baseband modulation and simple circuitry. This system represents first steps toward this, but demonstrates that systems with gigabit throughput are feasible.

ACKNOWLEDGMENT

The authors would like to acknowledge the contributions of their colleagues.

REFERENCES

[1] J. P. Javaudin, M. Bellec, D. Varoutas, and V. Suraci, “OMEGA ICT project: Towards convergent gigabit home networks,” in *Proc. IEEE 19th Int. Symp. Personal, Indoor and Mobile Radio Communications, 2008 (PIMRC 2008)*, pp. 1–5.

[2] J. Vucic, C. Kottke, S. Nerreter, A. Buttner, K. D. Langer, and J. W. Walewski, “White light wireless transmission at $200 + \mathrm{Mb}/s$ net data rate by use of discrete-multitone modulation,” *IEEE Photon. Technol. Lett.*, vol. 21, no. 20, pp. 1511–1513, Oct. 15, 2009.

[3] P. F. Szajowski, G. Nykolak, J. J. Auborn, H. M. Presby, G. E. Tourgee, E. Korevaar, J. Schuster, and I. I. Kim, “2.4 km free-space optical communication 1550 nm transmission link operating at 2.5 Gb/s—Experimental results,” in *Optical Wireless Communications*, 1999, pp. 29–40.

[4] G. Yun and M. Kavehrad, “Spot-diffusing and fly-eye receivers for indoor infrared wireless communications,” in *IEEE Proc. Int. Conf. Selected Topics Wireless Communications*, 1992, pp. 262–265.

[5] J. B. Carruthers and J. M. Kahn, “Angle diversity for nondirected wireless infrared communication,” *IEEE Trans. Commun.*, vol. 48, no. 6, pp. 960–969, Jun. 2000.

[6] D. C. O’Brien, G. E. Faulkner, E. B. Zyambo, K. Jim, D. J. Edwards, P. Stavrinou, G. Parry, J. Bellon, M. J. Sibley, V. A. Lalithambika, V. M. Joyner, R. J. Samsudin, D. M. Holburn, and R. J. Mears, “Integrated transceivers for optical wireless communications,” *IEEE J. Sel. Topics Quantum Electron.*, vol. 11, no. 1, pp. 173–183, Jan./Feb. 2005.

[7] O. Bouchet, M. E. Tabach, M. Wolf, D. C. O’Brien, G. E. Faulkner, J. W. Walewski, S. Randel, M. Franke, S. Nerreter, K. D. Langer, J. Grubor, and T. Kamalakis, “Hybrid wireless optics (HWO): Building the next-generation home network,” in *Proc. 6th Int. Symp. Communication Systems, Networks and Digital Processing, 2008 (CNSDSP 2008)*, pp. 283–287.